

Biochemica et Biophysica Acta, 464 (1977) 249–259
© Elsevier/North-Holland Biomedical Press

BBA 77576

AN ANALYSIS OF THE X-RAY INTERCHAIN PEAK PROFILE IN DIPALMITOYLGLYCEROPHOSPHOCHOLINE

GEORGE W. BRADY and DAVID B. FEIN

*Division of Laboratories and Research, New York State Department of Health, Albany,
N.Y. 12208 (U.S.A.)*

(Received July 5th, 1976)

Summary

The primary X-ray peak profile characterizing the interchain structure in the dipalmitoylglycerophosphocholine membrane has been measured as a function of temperature. The scattering between 23 and 34.6°C is characterized by an asymmetric crystalline reflection accounting for 85% of the total intensity, the remaining 15% being liquid-like in character. At a pre-transition temperature of 34.6°C, the reflection profile becomes (nearly) symmetrical, indicating a change in tilt angle of the chains with respect to the membrane surface. This change is accompanied by an increase of 20% in the amount of liquid-like scattering, indicating that the pre-transition mechanism includes a partial melting of the chains. At the melting point, 41.5°C, the crystalline reflection disappears, and the liquid component of the scattering increases to a point where it includes all the scattered intensity. The relative values of the integrated intensities at each temperature are tabulated, and the significance of the peak widths and shapes are discussed.

Introduction

The interchain scattering in phospholipids bilayers is characterized [1,2] by a peak, varying in sharpness and position with temperature. The position of the peak in *s* space is determined by the interchain spacing. At lower temperatures the chains appear to stack into a hexagonal array of rigid rods [1–3], as in a 2-dimensional crystalline lattice, while at higher temperatures the packing becomes disordered, a state more characteristic of liquid chains. There is a transition between the two states at a temperature T_c , the melting temperature, which depends on the chain length, the degree of chain branching and the extent of double bond character. A heat of 8.2 kcal/mol is associated with the

Abbreviation: DPPC, dipalmitoylglycerophosphocholine.

transition [4,5]. Below T_c there is another pre-transition temperature which is also characterized by a latent heat, about 0.2-times the magnitude of that at T_c . At this temperature there is a change in the angle of tilt of the chains with respect to the bilayer surface. Below the pre-transition temperature the chains appear to be tilted at an angle of $\approx 30^\circ$; above it they are normal to it. In dipalmitoylglycerophosphocholine, the relevant value for the pre-transition temperature is ≈ 34.6 and for the melting temperature T_c , $\approx 42.0^\circ\text{C}$. The Bragg interchain spacing below and above T_c are 4.16 and 4.6 Å, respectively. Other phases have been observed and have been classified by Tardieu and Luzzatti [1].

Many details of the bilayer structure are still unclear. The actual amount of structural order in the chains has not been established. Electron probe and NMR measurements indicate a considerable amount of rotational motion [6–9]. In fact, the EPR measurements are interpreted as showing that the chain order only persists to be about the seventh C atom, counted from the polar head group. A disturbing fact is that there is considerable difference between the high resolution NMR spectra for sonicated and unsonicated phospholipids. Further, the structural details in the region midway between the two surfaces, particularly [9] the degree of registry between hydrocarbon chain ends, have not been established [9]. This is an important consideration in the mechanism of lateral diffusion [10,11], where it is not clear how both halves of the bilayer take part cooperatively in the process; if there were registry, the interpretation would be simplified. Also, since sonicated vesicles are widely used as membrane model systems, the effect of curvature, which introduces the added complication of having to accommodate in the membrane structure two halves of different area, becomes a significant factor.

In this report we present results of the X-ray determination and analysis of the intensity profiles of suspensions of dipalmitoylglycerophosphocholine as a function of concentration and temperature. Surprisingly, no precise determination of the peak profile, properly corrected for solvent scattering, and including the intensity profile in the angular region to the left and right of the peak, has appeared so far in the literature. Since careful intensity comparison techniques [12,13] generally show features which are obscured when Fourier transform or deconvolution techniques are used, and since these features are revealing as to the physical state of the system, such a study is worthwhile. This is the first in a projected series of publications in which the contributions to the scattering of each membrane component and its correlation with the scattering from the other component, will be evaluated.

Experimental

The X-ray measurements were made in transmission goniometer, fitted with a LiF singly bent crystal monochromatic. A set of slits defined an area of 0.5 mm² at the sample. To eliminate air scattering, the X-ray path between the source and the counter was enclosed and helium flowed through it continuously. The sample was held in a cell whose windows were made of 5 mil beryllium metal. The cell was enclosed in a thermostat whose temperature could be varied between 34 and 100°C. The temperature control was accurate to 0.1°C. This

apparatus was designed to provide accurate intensity measurements in the correlation range from 1.5 to 50 Å and is particularly useful for measurements in the region of the interchain correlation distance. It has been fully described elsewhere [14]. Also described elsewhere [15] is the absorption correction technique, based on measuring the integrated intensity of the (10 $\bar{1}$) reflection from the cell windows, and from this computing the absorption correction at all angles. This technique is an important part of the procedure, since after these corrections are applied, the intensity patterns can be directly compared or subtracted one from the other, thus allowing isolation of the scattering contribution of the various components in the system.

The intensity patterns were measured with Cu K α radiation, by step-scanning in steps of 0.2° 2 Θ between 8 and 30° 2 Θ . Multiple scans were taken, and the data collected and averaged on a PDP8/E computer. 16 000 counts were collected for each step, and a least squares program averaged over 5 adjacent steps to give a probable error of 0.3% for each point. The scans were programmed so that different parts of the patterns were taken at different times. For example, the pattern between 16 and 30° would be recorded, then the pattern between 8 and 20° 2 Θ , in each case allowing sufficient overlap to ensure that no long term drift took place, or that no settling of the suspensions occurred (see below). Background corrections were negligible. Polarization corrections were applied. The intensities shown in the figures are plotted against s as abscissa ($s = 4\pi/\lambda \sin \Theta$, where λ is the wave length and Θ is one-half the scattering angle).

The intensities were scaled to the units of the scattering factors as follows: the scattering curve for pure H₂O was measured. This scattering is given by the expression

$$I_{\text{H}_2\text{O}} = F_{\text{H}_2\text{O}} + f_{\text{H}_2\text{O}}^2 \left[1 + 4\pi\rho \int_0^\infty r^2 \{g_{\text{H}_2\text{O}}(r) - 1\} \frac{\sin sr}{sr} dr \right] \quad (1)$$

where $f_{\text{H}_2\text{O}}$ and $F_{\text{H}_2\text{O}}$ are the coherent and incoherent scattering factors, respectively, for H₂O, and $g_{\text{H}_2\text{O}}(r)$ is the radial distribution function defined such that $4\pi r^2 g(r) dr$ gives the number of H₂O's in a spherical shell of radius r and thickness dr about each H₂O. The scattering factors are tabulated recording to James and Brindley [16]. The scaling can be conveniently done at any value of s where the integral term in Eq. 1 is zero. For H₂O a convenient value where this occurs is at $s = 1.76$ [17,18]. The measured intensity at $s = 1.76$ can be equated to $f_{\text{H}_2\text{O}}^2 + F_{\text{H}_2\text{O}}$, thus permitting the scattering factors to be expressed in the experimental units at all values of s . The integral term can then also be obtained from Eqn. 1 by difference.

Extending this procedure, the scattering factors for the dipalmitoylglycerophosphocholine component present in each solution can be evaluated. The scattering unit at each concentration is given by

$$(f_{\text{DPPC}}^2 + F_{\text{DPPC}})_x (f_{\text{H}_2\text{O}}^2 + F_{\text{H}_2\text{O}})_{1-x}$$

where x is the mole fraction of dipalmitoylglycerophosphocholine and the calculation of $(f_{\text{DPPC}}^2 + F_{\text{DPPC}})$ in the experimental units is straightforward; it is shown in Fig. 4. The advantage of this procedure is that the measured scattering can be corrected for incoherent scattering at all angles. In addition, it per-

mits the correction for the H_2O molecules bound to the polar head groups of the bilayer to be properly applied to $g_{\text{H}_2\text{O}}(r)$, rather than to $I_{\text{H}_2\text{O}}$ [12], thus taking account of the fact that the perturbing effect of the polar layers is felt in a partial breakdown of the solvent structure.

The compositions of the three solutions studied were 4.76, 6.25 and 9.09% dipalmitoylglycerophosphocholine weight. These will be referred to as solutions 1, 2 and 3. On a mole basis the compositions are:

Solution 1. $(\text{DPPC})_{0.001225}(\text{H}_2\text{O})_{0.9988}$,

Solution 2. $(\text{DPPC})_{0.001632}(\text{H}_2\text{O})_{0.9985}$,

Solution 3. $(\text{DPPC})_{0.002446}(\text{H}_2\text{O})_{0.9976}$.

From the chemical formula for dipalmitoylglycerophosphocholine, the concentrations for C in the three solutions are in the ratio of 1 : 1.27 : 1.76 when expressed in atomic fractions.

The H_2O scattering scaled to the appropriate concentration was subtracted from the measured curves after correction for bound H_2O was made. This was done by assigning a maximum of 10 to the number of H_2O molecules either bound directly to each polar head group or otherwise constrained by its electric field so that they could no longer be considered as part of the solvent continuum. This number is reasonable since there are two centres of ionic charge in the head group, each of which would affect at least one tetrahedral unit of the H_2O structure at the interface. At the highest concentration (solution 3), the mole ratio of polar groups to H_2O is only 0.0025, so that the assignment of 10 would only affect $\approx 2\%$ of the H_2O molecules. (Reducing the number to 5 did not qualitatively affect the results, although it led to ambiguities in the quantitative interpretation of the results. Making the physically untenable assumption that the solvent-head group interaction is negligible led to unreasonably high amounts of residual scattering on both sides of the peak profile, which did not correlate in any way with the dipalmitoylglycerophosphocholine concentration). The correction was made by reducing the integral term in Eqn. 1 by an amount proportional to the bound fraction H_2O [12]. Physically this implies a decrease in $g_{\text{H}_2\text{O}}(r)$, either because the nearest neighbor H_2O coordination is weakened by the reorienting effect of the surface groups, or because the bound molecules no longer are counted in the evaluation of $g_{\text{H}_2\text{O}}(r)$. Since the integral term in Eqn. 1 is negative and large out to $s = 1.76$, a decrease in $g_{\text{H}_2\text{O}}(r)$ leads to a significant increase in $I_{\text{H}_2\text{O}}$. The scattering of the bound H_2O is included in the calculation of the scattering factor. Thus the formula of the solution is modified to

$$[\text{DPPC}(\text{H}_2\text{O})_n^{\text{B}}]_x [\text{H}_2\text{O}]_{1-x-nx}$$

where n is the number of bound water molecules $(\text{H}_2\text{O})^{\text{B}}$. The scattering unit for DPPC is then

$$(f_{\text{DPPC}}^2 + nf_{\text{H}_2\text{O}}^2)_x (F_{\text{DPPC}} + nF_{\text{H}_2\text{O}})_x.$$

Research grade Supelco dipalmitoylglycerophosphocholine was used in all the experiments. The solutions were made up by evaporating off the CHCl_3 solvent in which the material was dissolved in a stream of N_2 , adding the

appropriate weight of H_2O and then alternately shaking the samples in a mechanical mixer and vortexing them for 30–60 min at 43°C . The dispersions thus prepared did not settle for periods of 24 h, and gave reproducible results over this period of time. The advantage of using such dilute solutions is that complete randomness is assured. For the sonication experiments, the dispersions were placed in a bath-type sonicator for 60 min at 43°C . After this treatment the samples had become opalescent and exhibited a bluish tinge.

Results and Discussion

The scattering curves for H_2O and for solution 2 are shown in Fig. 1. They are of interest in showing the effect of temperature, and to indicate the magnitude of the dipalmitoylglycerophosphocholine scattering relative to that of H_2O . The three states are easily distinguished. Below 35°C , the peak shows a considerable asymmetry on the right hand side. Above 35°C the scattering on the right of the peak has decreased markedly. The asymmetric properties of the two curves are characteristic of a (hk) reflection, uncorrelated in orientation or position in the l direction. Since hk planes are limited in the l direction by the finite length of the rigid hydrocarbon chains, the asymmetric tail, rather than being a diffuse continuous band, is terminated at a point in reciprocal space which is determined by the square of the Fourier transform of the rigid chain, and its angle of tilt relative to the plane of the bilayer. This fact will be discussed more fully below.

Above 42°C the peak has transformed into a broad band, whose maximum

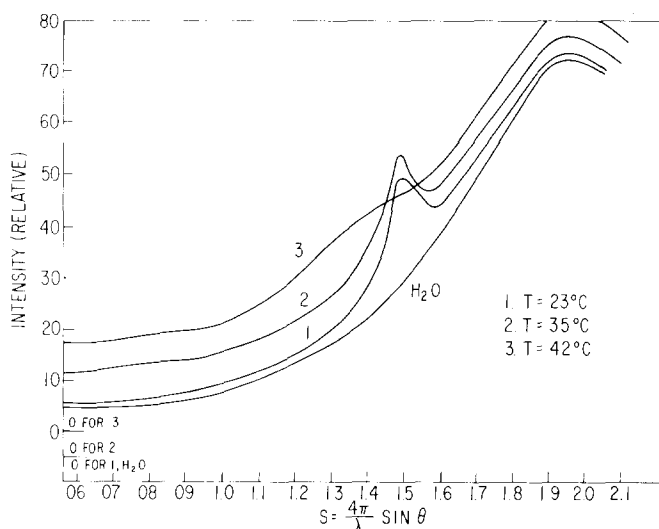


Fig. 1. Scattering curves for dipalmitoylglycerophosphocholine solution 2 and H_2O . The H_2O curve was measured at 23°C , and the temperatures for the dipalmitoylglycerophosphocholine curves are shown in the figure. Dipalmitoylglycerophosphocholine concentration is 6.25% by weight. Solutions 1 and 3 show similar curves. When the H_2O scattering is removed, as described in the text, the integrated areas of the total profiles for all three temperatures are in the ratio 1 : 1.30 : 1.80 for solution 1, 2, and 3, in agreement with the mole ratios of dipalmitoylglycerophosphocholine in the three solutions.

has shifted to a lower angle. Comparison with the H₂O curves shows that there is excess dipalmitoylglycerophosphocholine scattering at all angles.

The curves for solution 2, corrected for H₂O background and incoherent scattering are plotted in Fig. 2. The integrated areas under the three curves are the same (within experimental error) for the three temperatures; the values, in arbitrary units are 3031, 3100 and 3085 for curves 1, 2 and 3 respectively. The features of the curves are quite striking and show that the processes leading to complete "melting" are complex. There is no visible change in curve 1 between 23 and 34.6°C. To be noted is the presence of a faint, broad, liquid-like peak at $s = 0.78$, corresponding to a correlation distance of 9.9 Å. At this distance only head group correlations seem probable, and since the head group entity with excess electron density is the PO₄⁻ group, we identify the 9.9 Å distance with the spatial separation of these groups. The main peak maximum at $s = 1.51$ is of course identified with the Bragg spacing of 4.18 Å between the chains.

The abrupt change in the pattern between 34 and 35°C signals the appearance of a new state of organization of the chains, which persists unchanged (curve 2) until the "melting" point is reached at 41.5°C. The detail on the left and right of the main peak is now much more clearly displayed than in Fig. 1. There is little change in the position of the peak maximum. On the left, the increased scattering now takes the appearance of an unresolved band, while on the right the tail has decreased to such an extent that the peak profile has become nearly Gaussian in shape. The scattering in the region of $s = 0.78$ has intensified; in fact the curve in this region now appears to be the tail end of a band whose maximum is centered at a lower value of s , to the left of the range covered by our experiments.

At 41.5°C, the scattering is characterized by a single diffuse peak, showing asymmetry towards lower angle; the detail present in the lower temperature curves has disappeared, and a first conclusion would be that the scattering is now ascribable to a single state of chain organization, liquid-like in character. From the modified Debye equation

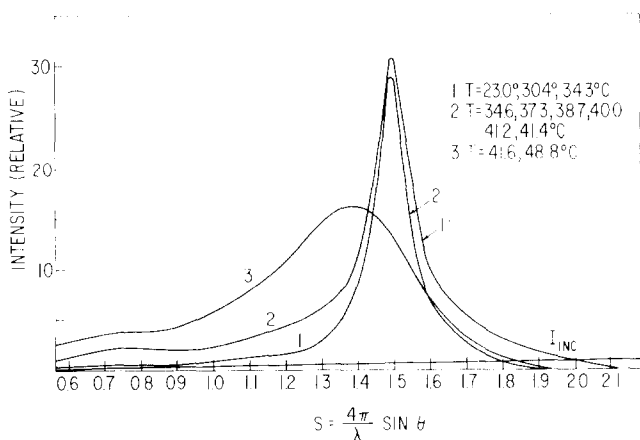


Fig. 2. The isolated dipalmitoylglycerophosphocholine coherent scattering as a function of temperature. Dipalmitoylglycerophosphocholine concentration, 6.25% by weight.

$$S_{\max}r = 7.72 \quad (2)$$

the mean interchain distance corresponding to $S_{\max} = 1.39$ is 5.56 \AA .

The curves in Fig. 2 are free of absorption and incoherent scattering, and their intensities are normalized to the units of the independent coherent scattering for dipalmitoylglycerophosphocholine, which is also shown in the figure. We can thus compare them with each other and use them to calculate the relative amounts of crystalline and liquid-like C-C bonds contributing to the curves in each temperature region. Implicit in this method of assessment is the assumption that the chain organization can be described by two states, an assumption based on the fact that the excess scattering on the left of the main peak in curves 1 and 2 can be reproduced, within experimental error, by curve 3, scaled down by an appropriate factor. The peak in curve 3 is broad enough to encompass a range of disordered structures, and therefore that state describing the liquid-like material is defined broadly enough to take account of this fact. The second state is defined more rigorously to mean that the material in it exists at each temperature in a single crystalline state. Such a definition is supported by the fact that at the 34.6°C pre-transition, in which there is an abrupt increase in the amount of liquid-like component, the crystalline peak does not broaden at all, which would be true if there were an increase in the disorder or variety of the crystalline states; in fact it narrows due to the diminution of the tail on the right hand side. Physically, the experiments do not as yet distinguish between a system in which there exist separate domains of ordered and disordered material, and one in which a portion of each chain is disordered. We tend to favor the latter, since it is difficult to see how such domains would be formed in the absence of a nucleation effect. A partial chain disorder, on the other hand, would result from an increased internal pressure at the interior of the bilayer, due to curvature, or from a cooperative effect between polar head group and interchain interactions, in which the former constrains the latter into a conformation in which the energy balance requires that a portion of the chain be disordered. Discussion of these effects, however, must remain speculative until the architecture of the head group layer is determined [19]. Janiak and coworkers, [20] in experiments with stacked layers, have observed the appearance of a new set of peaks in the small angle region at the pre-transition point, which is interpreted as being due to the development of a corrugated structure, with periodic ripples in the plane of the lamellae. Pinto da Silva [21] had also observed the same phenomenon in freeze-fracture electron microscope studies of dipalmitoylglycerophosphocholine. Our findings are compatible with these observations, because the transition to the rippled structure very likely is associated with the appearance of a new degree of dimensional flexibility in the chains; a partial liquefaction, at the hydrocarbon end of the molecule furnishes this.

The partition of the scattering between liquid and crystalline forms is accomplished by determining the scaling factors by which curve 3 must be multiplied so that it fits curves 1 and 2 at values of s between 1.1 and 1.2. This range is chosen because it is midway between the region at $s = 0.78$, where there is excess scattering, and the region of the main peak. In this way overlap from these two regions is minimized. It should be pointed out that the fit over this

range is quite good, and that moving the fitting range to lower or higher values of s has little effect on the results unless it clearly overlaps one or the other of these two regions. The decomposition is shown in Fig. 3. The peak areas, for curve 1, below the pre-transition temperature are 454 for the liquid component and 2567 for the crystalline peak. The percentage 15% of liquid-like intensity is real and significant, and it is tempting to ascribe it to a region of disorder in the vicinity of the terminal CH_3 group, involving only the first few atoms of the chain.

At the pre-transition temperature, there is a sharp increase of 20% in the amount of liquid scattering, accompanied by an equivalent decrease in the amount of crystalline scattering; the peak area values are now 1080 and 2020 for the two types. The leading edge of the reflection has been sharpened to both temperatures; the asymmetric tail in the room temperature (23°C) curve has become even more pronounced relative to the curve above 34.6°C . The increase of 20% in the amount of liquid component at the pre-transition, relative to the value of 100% at the melting transition is to be compared to the corresponding values of the heats of transition at the two temperatures; the values for these, measured calorimetrically by Suurkuusk et al. [22] are 1.6 and 8.2 kcal respectively, also in the ratio of 1:5.

With reference to the change in tilt angle of the chains at the pre-transition temperature, we note that measurements of the bilayer repeat distance by Rand et al. [23] show that at the pre-transition this distance increases from $64.2 \pm 0.2 \text{ \AA}$ to $70.0 \pm 0.8 \text{ \AA}$. If the transition mechanism involved only a simple rotation of rigid chains, for a change in tilt angle of 30° , an increase to 74.1 \AA would be predicted. The fact that our results show that the mechanism is accompanied with a considerable amount of partial "melting" explains this discrepancy, because the end-to-end distance of a disordered chain, or of a

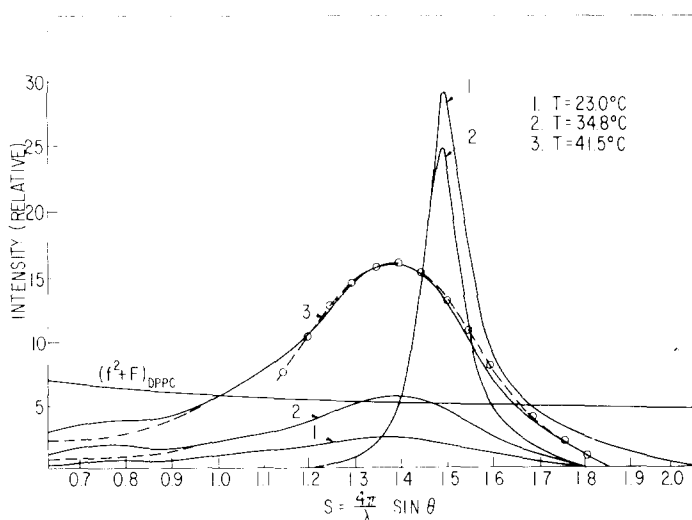


Fig. 3. The curves of Fig. 3 resolved into liquid-like and crystalline components. The dashed curve is for a liquid characterized by only one distance. See text.

chain in which a portion of it is disordered, would be significantly less. Using techniques developed in previous measurements on disordered alkane chains [24], a good estimate of the end-to-end decrease could be made but this would require a knowledge of the state of registry, if any, between chain ends. In the absence of this, an exact correlation between the change in bilayer dimensions and the increased degree of chain disorder is not feasible. Qualitatively though, the two observations complement each other.

As concerns the angle of tilt and its effect on the asymmetry of the peak profile, this results because in reciprocal space the position and shape are determined by the reciprocal vectors ha^* and kb^* , characterizing the interchain distance, and the square of Fourier transform of the rigid chain projected along a line in the c^* direction [1,2]. For $h = k = 1$ the equation of the line is $s = a^* + b^* + \alpha c^*$, where α is a continuous variable. For infinitely long chains, α is unity and the line reduces to a point, to give a unique value for s . For finite, perpendicularly oriented chains, the projection is centered symmetrically around the point $\alpha = 0$ on the line, becoming broader as the chains shorten. For tilted chains the projection is shifted to another value of α which is determined by the cosine of the angle of tilt. In real space this corresponds to a shift of the projection of the electron density of the rod on the bilayer plane. The angle of tilt can be estimated from the ratio of the values of s at which the tails of the reflection terminate; these are 1.83 \AA^{-1} and 2.11 \AA^{-1} for curve 2 (36°C) and curve 1 (23°C) respectively. The ratio $1.83/2.11 = \cos \phi = 0.867$, which gives 29° for the angle of tilt ϕ . The calculation pre-supposes that the Fourier transforms of the chains in the two states are not significantly different, and the accuracy of the estimated value is conditional on the extent to which this assumption is valid.

Finally, since curve 3 in Fig. 3 is the scattering from a system of liquid chains, it can be represented by the equation

$$I_{cc} = f_c^2 \left[1 + 4\pi\rho \int_0^\infty r^2 \{g_{cc}(r) - 1\} \frac{\sin sr}{sr} dr \right] \quad (3)$$

analogous to Eqn. 1, with f_c and g_{cc} being the scattering factor and the radial distribution function for the C atoms respectively. The integral term is given by the difference between the measured intensity and f_{cc}^2 ; its form is determined by $g_{cc}(r)$ and from this we can estimate the breadth of the nearest neighbor C-C distance distribution between chains. As a starting point, we can choose a δ -function for $g(r)$, with a non-zero value at $r_0 = 5.56 \text{ \AA}$. The integral then reduces to an expression whose s dependence is determined by $r_2^0 (\sin sr_0/sr_0)$, this function normalized at the peak maximum is plotted in Fig. 4. It can be seen that the single distance distribution approximates the measured intensity curve quite well. This is not in general true for a liquid system, and while such a result is not to be construed as indicating that there is only one C-C distance on the average, it does show that the motional characteristics of the membrane chains are of a much more restricted nature than those appropriate to a system of the same chains possessing all the degrees of freedom of a free liquid. This is in large measure due to the fact that translational motion is restricted to 2 dimensions, and thus the free volume available to each molecule is less. Also the sliding mo-

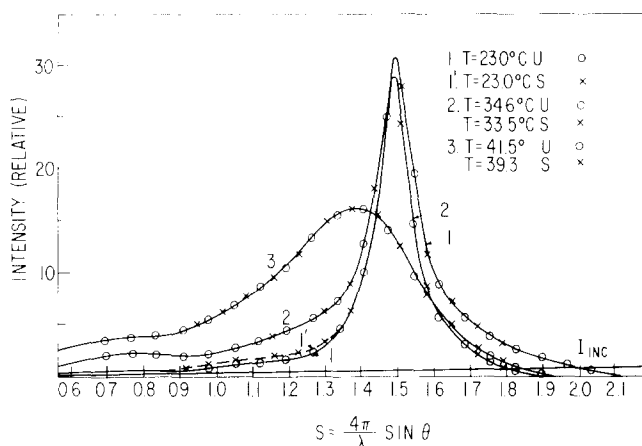


Fig. 4. Comparison curves for unsonicated and sonicated solutions. Only a representative number (40%) of the actual experimental points are plotted.

tion of one chain with respect to another is constrained by the strong attraction between the polar head group and the external water phase, which tend to restrict this motion to an oscillation of the C atoms in one chain with respect to those in adjacent chains.

Effect of sonication

To determine the effect of curvature on the chain organization, it was of interest to compare the scattering curves obtained in the Bangham type bilayers with those obtained on sonicated bilayers, under equivalent concentration and ionic strength conditions. No electrolyte was added in either set of experiments, because this would have markedly affected the H₂O background correction [12]. Also, we wished to avoid the instability effects observed by Suurkuusk et al. [22], ascribed by them to agglomeration of the very small (≈ 100 Å) vesicles which are obtained when the Huang and Thompson procedure [25] is used. The sonication was stopped after the samples became semi-transparent. They were then stored at room temperature under N₂ for 24 h before the measurements were made. No attempt was made to fractionate the vesicles. The experiments are thus of a preliminary nature, but seem interesting enough to warrant a brief inclusion.

Fig. 4 shows the scattering curves for the two types of systems for different temperatures. It is seen that the curves are in general quite similar, except that both the pre-transition and the transition temperatures are lowered significantly. The pre-transition temperature has dropped to 33.5°C and the melting transition now appears at 39.3°C. The 33.5°C curve shows a slight increase, about 2%, in the liquid region relative to the 34.6°C curve for unsonicated samples. We conclude from these measurements that the fundamental organization of the chains is not affected by sonication, but that the chain structure at any temperature in unsonicated membranes will appear at a lower temperature in the sonicated membranes. This fact has importance in a practical sense, because we found that sonicated dispersed systems gave stable

results for periods of time roughly twice as long as those for unsonicated samples. Sonicated samples are also less viscous; the consequent increased ease of manipulation makes their use worthwhile. It is interesting to speculate that severe sonication could lead to a condition where the pre-transition phenomenon is eliminated, and that the increased amount of liquid-like chain structure will be present at all temperatures below T_c . Further experiments will be done to see whether this is true.

Acknowledgments

We would like to thank D. Papahadjopoulos for his assistance and advice in preparing the samples. We thank D. Engelman for a stimulating discussion on membrane scattering.

References

- 1 Tardieu, A., Luzzati, V. and Reman, F.C. (1973) *J. Mol. Biol.* 75, 711–733
- 2 Chapman, D., Williams, R.M. and Ladbroke, B.D. (1967) *Chem. Phys. Lipids* 1, 445–475
- 3 Papahadjopoulos, D., Jacobsen, K., Nir, S. and Isaac, T. (1973) *Biochim. Biophys. Acta* 311, 330–348
- 4 Ladbroke, B.D. and Chapman, D. (1969) *Chem. Phys. Lipids* 3, 304–367
- 5 Hubbell, W.L. and McConnell, H.M. (1971) *J. Am. Chem. Soc.* 93, 314–326
- 6 Lee, A.C., Birdsall, N.S.M., Levine, Y.K. and Metcalfe, J.C. (1972) *Biochim. Biophys. Acta*, 255, 43–56
- 7 Oldfield, E., Chapman, D. and Derbyshire, W. (1971) *FEBS Lett.* 23, 285–297
- 8 Seeling, J. and Seeling, A. (1974) *Biochim. Biophys. Res. Commun.* 57, 406–407
- 9 Wilkins, M.H.F., Blaurock, A.E. and Engelman, D.M. (1971) *Nat. New Biol.* 230, 72–76
- 10 Kornberg, R.D. and McConnell, H.M. (1971). *Proc. Natl. Acad. Sci.* 68, 2564–2568
- 11 Chapman, D. (1975) *Q. Rev. Biophysics* 8, 185–235
- 12 Brady, G. W. and Kaplan, M.L. (1973) *J. Chem. Phys.* 58, 3535–3541
- 13 Brady, G.W. (1974) *J. Chem. Phys.* 60, 3466–3473
- 14 Brady, G.W. and Greenfield, A.J. (1967) *Rev. Sci. Instrum.* 38, 736–739
- 15 Brady, G.W., Cohen-Addad, C. and Lyden, E.F.X. (1969) *J. Chem. Phys.* 51, 4309–4319
- 16 James, R.W. and Brindley, G.W. (1931). *Z. Kristall* 78, 470–485
- 17 Brady, G.W. and Romanow, W.J. (1960). *J. Chem. Phys.* 32, 306
- 18 Narten, A.H., Danford, M.D. and Levy, H.A. (1967) *Disc. Farad Soc.* 43, 97–106
- 19 Hitchcock, P.B., Mason, R. and Shipley, G.G. (1975) *J. Mol. Biol.* 94, 297–298
- 20 Janiak, M., Small, D. and Shipley, G.C. (1976) *Biochemistry*, in the press.
- 21 Pinto da Silva, P. (1971) *J. De Microsc.* 12, 185–189
- 22 Suurkuusk, J., Lentz, B.R., Barenholz, Y., Biltonen, R.L. and Thompson, T.E. (1976) *Biochemistry* 15, 1393–1401
- 23 Rand, R.P., Chapman, D. and Larsson, K. (1975) *Biophys. J.* 15, 1117–1123
- 24 Brady, G.W. and Fein, D.B. (1975). *J. App. Cryst.* 8, 261–265
- 25 Huang, C. and Thompson, T.E. (1974). *Methods Enzymol. Biomembranes* 32, 485–489